

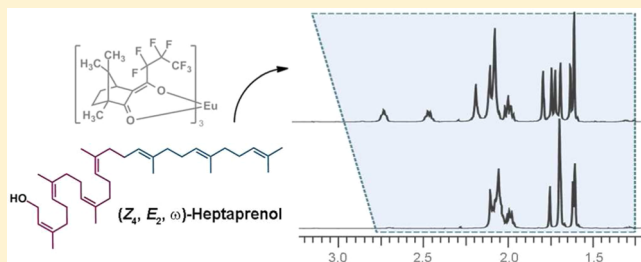
# Synthesis and NMR Characterization of (Z,Z,Z,Z,E,E, $\omega$ )-Heptaprenol

Dusan Heseck, Mijoon Lee, Jaroslav Zajíček, Jed F. Fisher, and Shahriar Mobashery\*

Department of Chemistry and Biochemistry, University of Notre Dame, Notre Dame, Indiana 46556, United States

**S** Supporting Information

**ABSTRACT:** We describe a practical, multigram synthesis of (2Z,6Z,10Z,14Z,18E,22E)-3,7,11,15,19,23,27-heptamethyl-2,6,10,14,18,22,26-octacosaeptaen-1-ol [(Z<sub>4</sub>E<sub>2</sub> $\omega$ )-heptaprenol, **4**] using the nerol-derived sulfone **8** as the key intermediate. Sulfone **8** is prepared by the literature route and is converted in five additional steps (18% yield from **8**) to (Z<sub>4</sub>E<sub>2</sub> $\omega$ )-heptaprenol **4**. The use of Eu(hfc)<sub>3</sub> as an NMR shift reagent not only enabled confirmation of the structure and stereochemistry of **4**, but further enabled the structural assignment to a major side product from a failed synthetic connection. The availability by this synthesis of (Z<sub>4</sub>E<sub>2</sub> $\omega$ )-heptaprenol **4** in gram quantities will enable preparative access to key reagents for the study of the biosynthesis of the bacterial cell envelope.



## INTRODUCTION

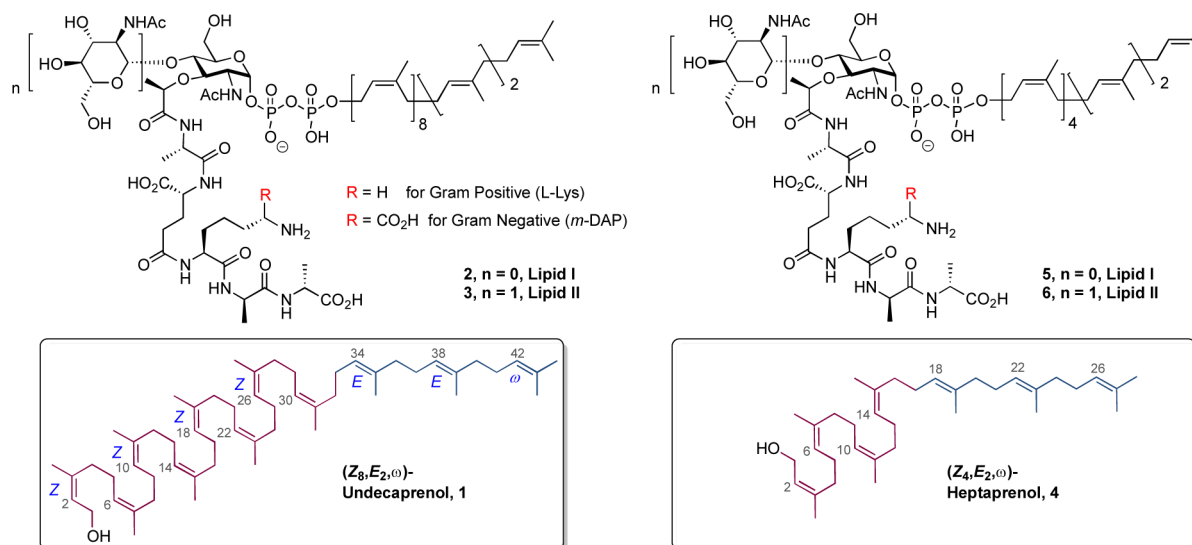
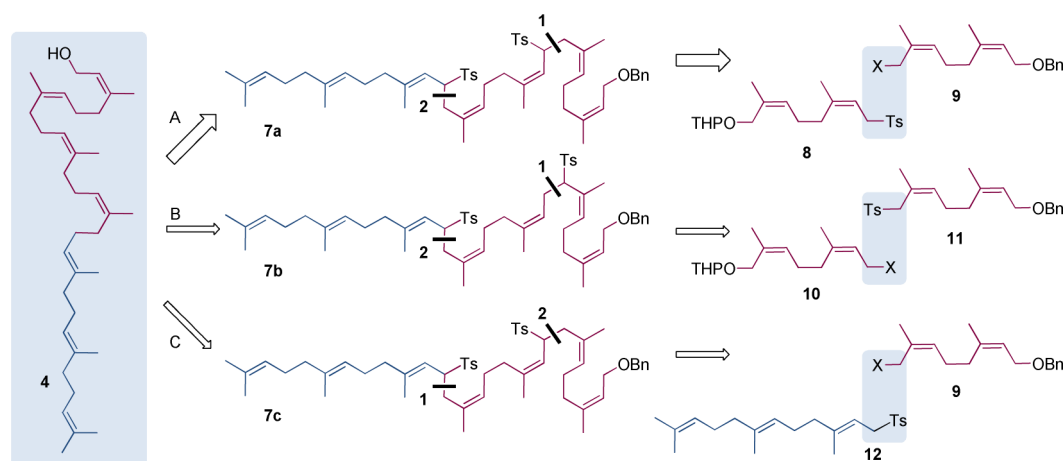
The five-carbon isoprene segment is foundational to the biosynthetic pathways of both primary and secondary metabolism.<sup>1</sup> One class of isoprenoids, the polyprenols, is used catalytically in primary metabolism as a membrane-integral carrier of hydrophilic structure: of the wall teichoic acids in Gram-positive bacteria; of the saccharides destined for the lipopolysaccharide of the outer membrane of Gram-negative bacteria; of the peptidoglycan monomers used by bacteria to assemble their cell wall; and of the saccharides destined for post-translational modification of prokaryotic and eukaryotic proteins.<sup>2,3</sup> The discovery in 1964 that a lipid intermediate was required for bacterial peptidoglycan synthesis<sup>4,5</sup> was followed in 1967 by its identification as a C<sub>55</sub> undecaprenol containing 11 C=C double bond functional groups.<sup>6–8</sup> As a result of the extensive overlap of resonances in the polyprenols,<sup>9</sup> the stereochemical assignment to the bacterial undecaprenol as the (Z<sub>8</sub>E<sub>2</sub> $\omega$ )-undecaenol [(2Z,6Z,10Z,14Z,18Z,22Z,26Z,30Z,34E,38E,42)-3,7,11,15,19,23,27,31,35,39,43-undecamethyl-2,6,10,14,18,22,26,30,34,38,42-tetratetracontaundecaen-1-ol, compound **1** in Chart 1] rests upon exquisite mechanistic studies pertaining to its biosynthesis. These studies show that a single enzyme, undecaprenol diphosphate synthase, synthesizes the diphosphate of **1** from farnesyl diphosphate by eight-fold *cis*-prenyl homologation using isopentenyl diphosphate as the prenyl donor.<sup>10–13</sup>

Nonetheless, the low pool levels of the bacterial lipid intermediates,<sup>14</sup> their limited accumulation in cell-free systems, and the tedious effort involved in their isolation and purification have restricted their availability for the study of the peptidoglycan pathway.<sup>15</sup> Several efforts toward the synthesis of the Lipid I, II, and IV structures and their analogues, using both chemical and chemoenzymatic methods, have been reported.<sup>15–22</sup> These syntheses are demanding, and indeed

several pivotal Lipid I/II structures (**2** and **3** in Chart 1), such as those having the *meso*-diaminopimelic substructure characteristic of Gram-negative Lipid II, have yet to be completed. Moreover, syntheses of prenol-containing structures often use the plant-derived (Z<sub>7</sub>E<sub>3</sub> $\omega$ )-undecaprenol as the lipid component. While the evidence thus far indicates that the (Z<sub>7</sub>E<sub>3</sub> $\omega$ )-undecaprenol and (Z<sub>8</sub>E<sub>2</sub> $\omega$ )-undecaprenol are functionally equivalent as the lipid component of Lipid II, these plant polyprenols are themselves rare. Given the important role of the lipid component in many aspects of biological recognition<sup>17</sup> and the scarcity of the natural polyprenols, the development of practical synthetic routes to these structures is important. The chemical synthesis of oligo- and polyprenols for use in prenol-containing structures is recent.<sup>23,24</sup> Previous syntheses of polyprenols include dolichol-20,<sup>25</sup> (Z<sub>8</sub>E<sub>2</sub> $\omega$ )-undecaprenol,<sup>26</sup> (Z<sub>7</sub>E<sub>3</sub> $\omega$ )-undecaprenol,<sup>27</sup> and (Z<sub>4</sub>E<sub>2</sub> $\omega$ )-heptaprenol.<sup>24,26,28</sup>

Walker, Kahne, and colleagues<sup>19,20</sup> showed that the Lipid II analogue **6**, having the shorter C<sub>35</sub> (Z<sub>4</sub>E<sub>2</sub> $\omega$ )-heptaprenol (Chart 1), is accepted *in vitro* as a component of the Lipid II substrate of the penicillin-binding protein (PBP) enzymes. Accordingly, a general synthesis of heptaprenols—and no less importantly, a versatile spectroscopic means of confirming their structure—would be especially useful. As a demonstration of both of these objectives, we report the synthesis of (2Z,6Z,10Z,14Z,18E,22E)-3,7,11,15,19,23,27-heptamethyl-2,6,10,14,18,22,26-octacosaeptaen-1-ol (Z<sub>4</sub>E<sub>2</sub> $\omega$ )-heptaprenol (**4**) and its complete <sup>1</sup>H and <sup>13</sup>C NMR assignment using chiral shift reagent-facilitated analysis of its homo- and heteronuclear 2D spectra.

**Received:** June 25, 2012

**Chart 1. Structures of the Undecaprenol-Containing Lipid I and Lipid II Used in Bacterial Peptidoglycan Biosynthesis and Their Heptaprenol Analogues****Scheme 1. Retrosynthetic Disconnections Evaluated as a Practical Synthesis of (Z<sub>4</sub>,E<sub>2</sub>,ω)-Heptaprenol**

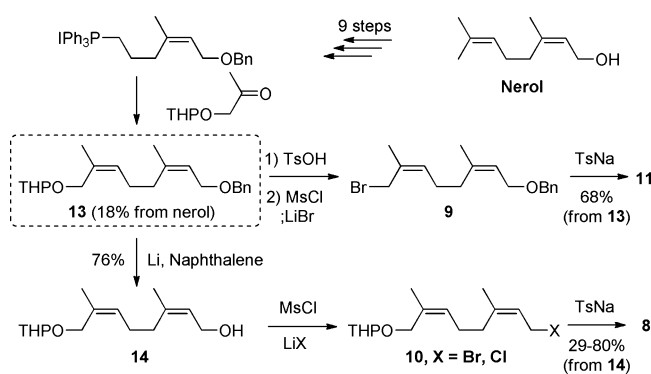
## RESULTS AND DISCUSSION

Three different retrosynthetic disconnections toward **4** were considered, corresponding to structures **7a**, **7b**, and **7c** as key intermediates (Scheme 1). These three intermediates coincide with the reaction of different sulfone-stabilized carbanions (**8**, **11**, and **12**) with a diprenyl halide (**9** or **10**, X = Cl, Br). Although the use of sulfone-stabilized carbanions is a standard method for polyprenol synthesis, a systematic evaluation of the most suitable reaction pairing in terms of yield and stereochemical fidelity was absent from the literature. The most frequently used route is **A** of Scheme 1. Our interest in the alternative routes **B** and **C** emerged from our recognition, as we examined these reactions, that the reagent pair **10** and **11** was easier to prepare on scale than the reagent pair **8** and **9**. While routes **A** and **B** synthesize the Z<sub>4</sub>-tetraprenol for coupling with the E<sub>2</sub>E-farnesol-derived sulfone **12**, route **C** reacts **12** with the nerol-derived halide **9**, followed by a second addition of **9** to complete the synthesis. Routes **A** and **C** have the advantage of using the most readily prepared neryl reagent (**9**, compared to the three other neryl derivatives **8**, **10**, and **11** shown in Scheme 2) as a starting material, but route **C** is disadvantaged relative to routes **A** and **B** by its requirement for two separate

desulfonation reactions (see Scheme 3, **22** to **23** and **7c** to **4C**).

We converted (commercially available) nerol to the pivotal intermediate **13** in 10 steps (including epoxide formation from the bromohydrin, epoxide hydrolysis, oxidative cleavage, reduction, iodination, triphenylphosphonium iodide formation, and Wittig reaction with the hydroxyketone) using the literature route.<sup>29</sup> Although this route appears laborious, it is quite amenable to scale (we have prepared **13** on a 50-g scale). Compound **13** was separately transformed into the four neryl derivatives (**8**–**11**) of Scheme 2. The syntheses of **9** and **11** were straightforward; the syntheses of **8** and **10** were not. The synthesis of sulfone **8** ultimately involved comparison of two different halides (**10-Br** and **10-Cl**) for the sulfone alkylation (see Figure 1, left side). Using **10-Br** as a reagent, we isolated **8** as the major product. In contrast, the analogous reaction using **10-Cl** as a reagent gave a 5:4 diastereomeric mixture of **8** and **15** as assessed by <sup>1</sup>H NMR analysis. These structures were assigned by extensive NMR analyses, done after removal of the *O*-THP protecting group in order to both simplify the NMR spectra and facilitate chromatographic purification.

## Scheme 2. Syntheses of the Four Neryl Units 8–11

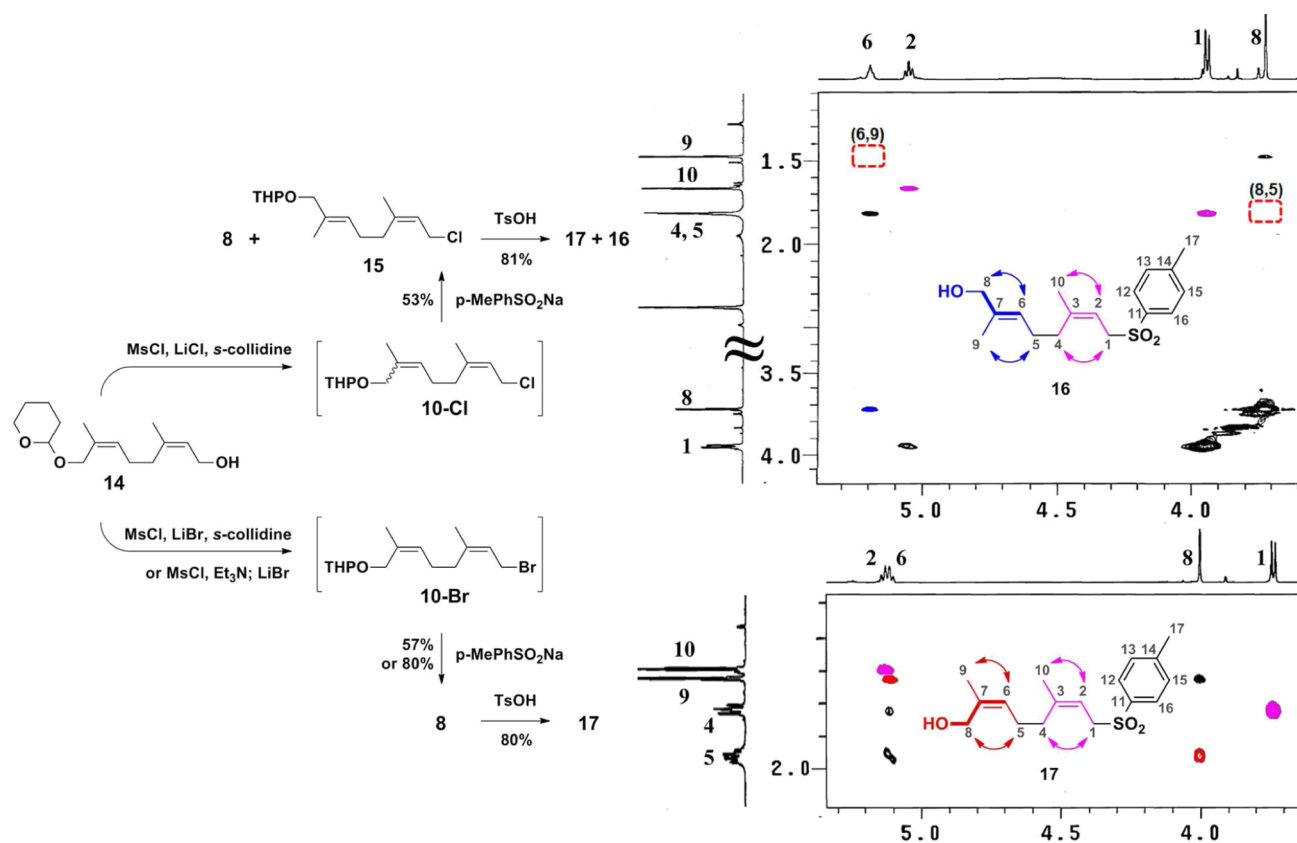


The  $^1\text{H}$  and  $^{13}\text{C}$  spectra of alcohols **17** (from **8**) and **16** (from **15**) are too similar to allow definitive structural assignment by themselves. Following resonance assignments from 2D homo- and heteronuclear correlation spectra, analysis of the corresponding ROESY spectra (Figure 1) identified the difference. Compound **17** (arising from reaction with **10-Br**) had the desired (*2Z,6Z*) stereochemistry, whereas **16** (from reaction with **10-Cl**) was the (*2Z,6E*)-stereoisomer. While *E,Z* scrambling is well known to occur during the synthesis of many allyl halides from allyl alcohols, we are at a loss to suggest the critical experimental difference accounting for the contrast between **10-Br** and **10-Cl**, and as well as to account for the unanticipated regiochemistry of the isomerization. Nonetheless, the discovery of this unexpectedly facile (and reproducible)

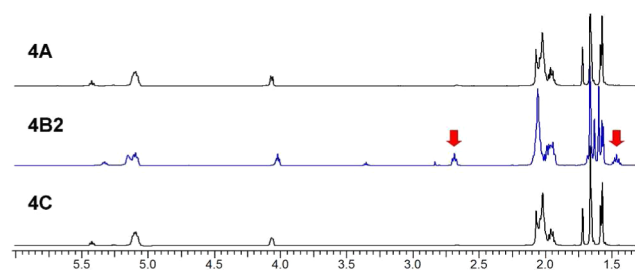
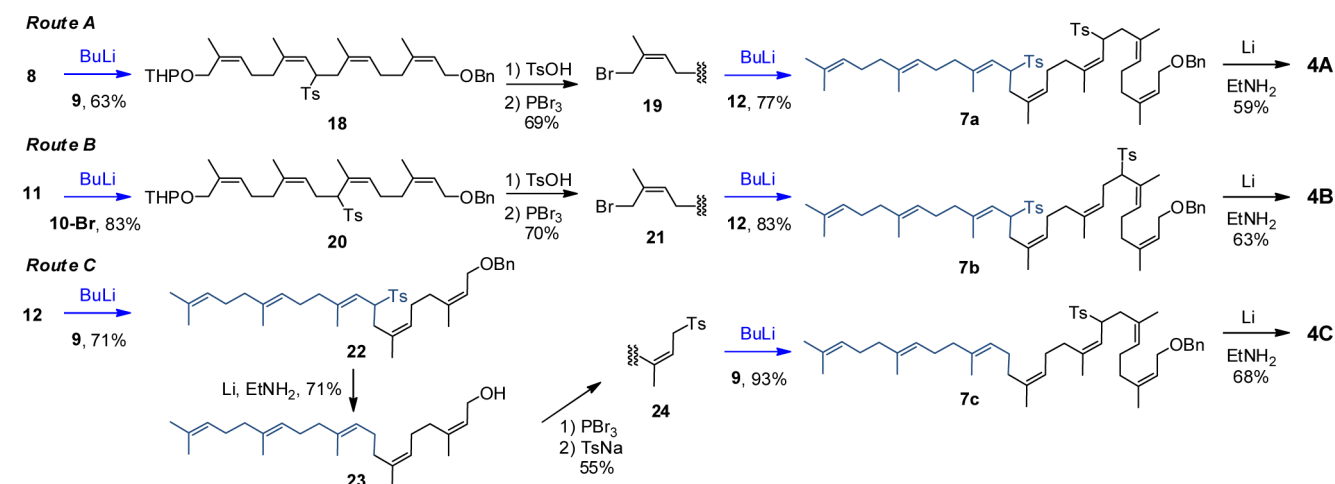
isomerization under one set of standard halogenation conditions, but not under another, set the requirement for full verification of structure and stereochemistry, following each key step of our synthesis.

From **8**, three routes toward heptaprenol **4** were compared (Scheme 3). Routes *A* and *B* used different neryl derivatives to give the nerylneryl derivative **18** (route *A*) and nerylneryl derivative **20** (route *B*), respectively. Each was separately coupled with farnesylsulfone **12**. Route *C* used repetitive coupling of neryl derivative **9**. In contrast to the final prenol structures, the penultimate synthetic intermediates give well-dispersed and easily interpretable NMR spectra, as exemplified by the complete assignment of **18-OH**, **20-OH**, and **7b** (**18-OH** was obtained after removal of *O*-THP in **18**, Supporting Information). Last, intermediates **7a**, **7b**, and **7c** were deprotected by sequential reductive desulfonation and reductive debenzoylation to give **4** (identified in Scheme 3 by their routes of synthesis: **4A**, **4B**, and **4C**).

The final products **4A** and **4C** gave identical  $^1\text{H}$  NMR spectra, characterized by eight methyl resonances in a 4:2:1 *Z/E/w* pattern (Figure 2). Further NMR analysis (see below) verified the product stereochemistry as the desired (*Z<sub>4</sub>E<sub>2</sub>w*)-heptaprenol **4**. The purity of the heptaprenol **4** isolated by silica flash chromatography (following the reductive desulfonation step) exceeded 90% by  $^1\text{H}$  NMR analysis (Supporting Information). The analytical data for **4** matched the published data given by Chang et al.<sup>28</sup> In contrast, the heptaprenol from route *B* was a 1:3 diastereomeric mixture of **4** and an isomer designated **4B2**. The mixture was separated by column

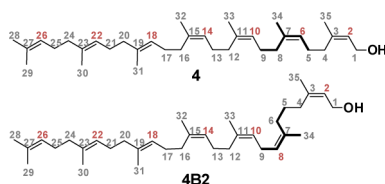


**Figure 1.** Key correlations in the  $^1\text{H}$  ROESY NMR spectra used to assign the alcohol diastereomers **16** (top spectrum) and **17** (bottom spectrum). Empty boxes in top spectrum indicate the absence of correlations from *6Z* (H-6,H-9) and (H-5,H-8). Instead, the ROESY spectrum for **16** shows correlation between H-6 and H-8 (colored in blue), demonstrating *6E* configuration. Relevant synthetic transformations are summarized on the left.

Scheme 3. Synthetic Routes Evaluated as a Practical Synthesis of the (*Z*<sub>4</sub>,*E*<sub>2</sub>,*ω*)-Heptaprenol

**Figure 2.** Comparison of  $^1\text{H}$  NMR spectra (500 MHz) of the heptaprenol isomers **4A**, **4B2**, and **4C** in  $\text{CDCl}_3$ .

chromatography. Although the  $^1\text{H}$  NMR spectra of **4** and **4B2** are very similar (and show extensive overlap of signals), the  $^1\text{H}$  spectrum of **4B2** has two distinguishing resonances (Figure 2, red arrows). These new resonances are diagnostic of an undesirable isomerization.



The extensive resonance overlaps for **4** and **4B2**, and the requirement for a definitive verification of the structure of **4**, prompted a search for a general NMR method to facilitate the structural assignment of prenyl derivatives. Proof of structure by NMR of a polyprenol (and of the synthetic intermediates leading to the polyprenol) is rare. Indeed, there is a 45-year gap between the discovery of polyprenol involvement in bacterial primary metabolism and a full NMR-based structural assignment of a polyprenol, that of the plant-derived (*Z*<sub>6</sub>,*E*<sub>3</sub>,*ω*)-decaprenol [(2*Z*,6*Z*,10*Z*,14*Z*,18*Z*,22*Z*,26*E*,30*E*,34*E*,38)-3,7,11,15,19,23,27,31,35,39-decamethyl-2,6,10,14,18,22,26,30,34,38-tetracontadecaen-1-ol] accomplished in 2009 using 3D NMR spectral analyses.<sup>30</sup> The absence of this characterization is understandable, due to the extensive overlap of resonances even at high magnetic field (~18.79 T). Nonetheless (and to our very pleasant surprise), an exploration of several common chiral shift reagents (including  $\text{Eu}(\text{tcf})_3$ ,  $\text{Eu}(\text{hcf})_3$ ,  $\text{Pr}(\text{hcf})_3$ ,  $\text{Yt}(\text{hcf})_3$ , and Resolve- $\text{Al AgFOD}$ ) demonstrated promise. Of these reagents,  $\text{Eu}(\text{hcf})_3$

was best. The use of chiral shifts to disperse the resonances of terpenoids for the purpose of structure assignment<sup>31,32</sup> or for enantiomeric ratio determination<sup>33–36</sup> is known, but infrequent. Optimization of the molar ratio of  $\text{Eu}(\text{hcf})_3$  to **4** for the purpose of structure assignment is shown in Figure 3. The

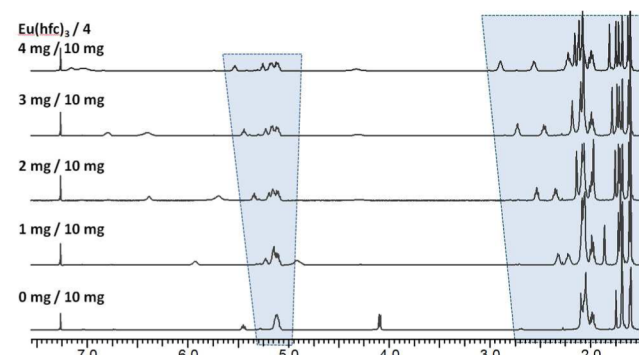


**Figure 3.**  $^1\text{H}$  NMR spectra (500 MHz) of **4** in the presence of different molar ratios of  $\text{Eu}(\text{hcf})_3$  (from bottom to top, molar ratios of 0, 0.04, 0.09, 0.13, and 0.17 equiv of shift agent to **4**). The optimal balance between resonance dispersion and line broadening occurs at 0.13 equiv of  $\text{Eu}(\text{hcf})_3$  (3 mg of  $\text{Eu}(\text{hcf})_3$  to 10 mg of **4** in  $\text{CDCl}_3$ ).

structure of heptaprenol **4** was verified by analysis of homonuclear (DQF-COSY, TOCSY, ROESY) and heteronuclear ( $^1\text{H}$ - $^{13}\text{C}$  HSQC, HSQC-TOCSY, HMBC) spectra obtained using 0.13 equiv of  $\text{Eu}(\text{hcf})_3$  to disperse the  $^1\text{H}$  resonances.  $^1\text{H}$  connectivities were established by analysis of the DQF-COSY and TOCSY spectra.

Resonances of all carbons with directly attached protons were assigned using the HSQC and HSQC-TOCSY spectra. For example, Figure 4A shows the correlation of the vinyl hydrogen and carbon resonances in the HSQC-TOCSY spectrum. The HMBC spectrum was then employed to assign the quaternary carbon resonances and to verify the correctness of the connectivities established by the analysis of the other spectra. Figure 4B shows the connectivities of the first two prenyl units (colored orange and turquoise, respectively) deduced from the HMBC spectrum. The H-5 resonance is identified in the HMBC spectrum by its correlation with the three carbon resonances (C-4, C-6, and C-7) of its prenyl unit (colored in turquoise), and by its additional correlation with

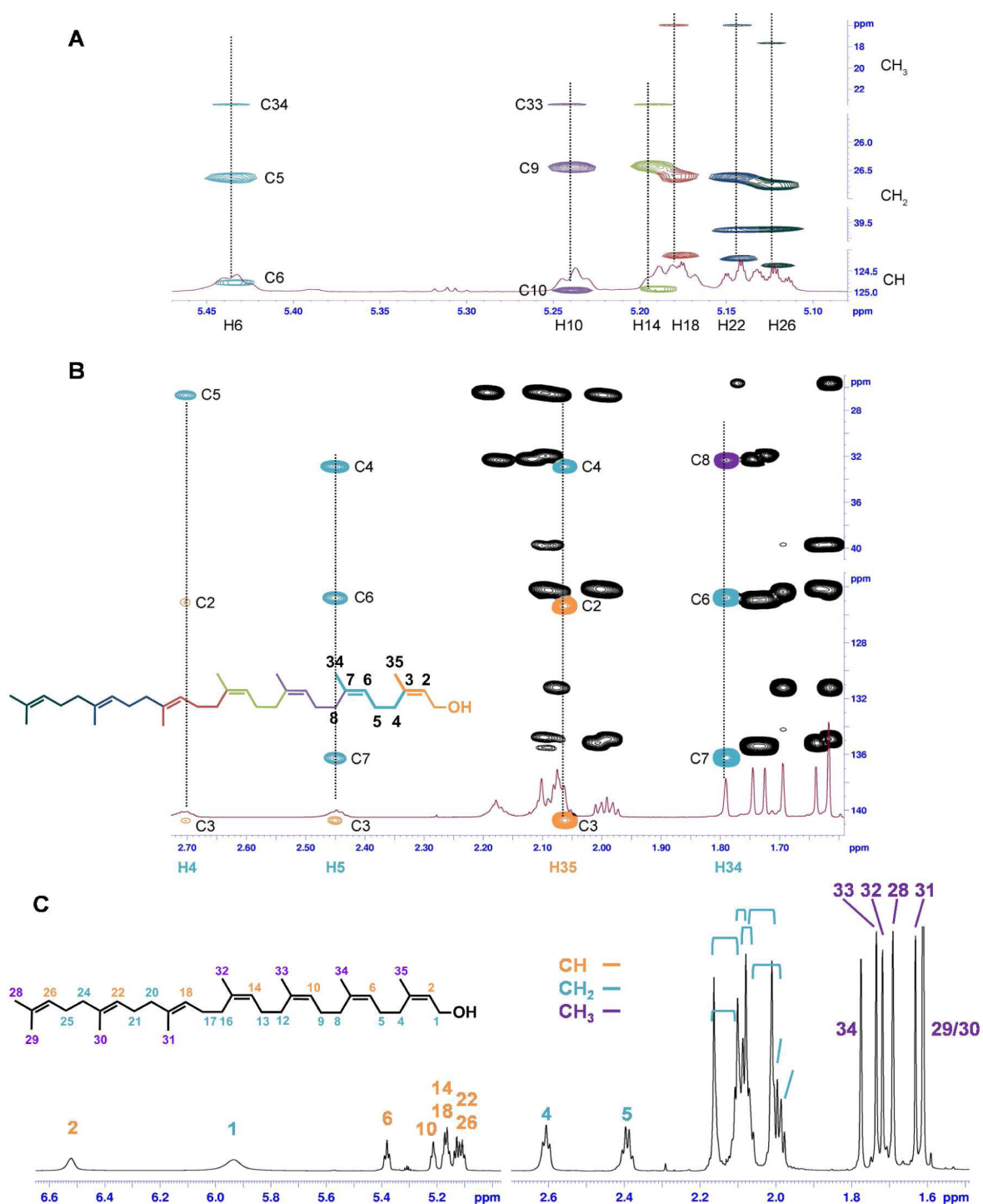


**Figure 4.** (A) Use of the HSQC-TOCSY spectrum for  $^{13}\text{C}$  ( $\text{CH}_3$ ,  $\text{CH}_2$ , and  $\text{CH}$ ) resonance correlation. Each prenyl unit is shown in a different color. (B) Interpretive use of the HBMCM exemplified by the correlations for the two terminal prenyl units (colored orange and turquoise). (C) Pictorial summary of the  $^1\text{H}$  resonance assignments for 4 (800.13 MHz spectrum, obtained using a solution of 10 mg of 4 and 3 mg of  $\text{Eu}(\text{hcf})_3$  in 600  $\mu\text{L}$  of  $\text{CDCl}_3$ ).

the C-3 signal of the neighboring prenyl unit (colored orange). The H-4 resonance also correlates with the C-2 and C-3 resonances from the neighboring prenyl unit (colored orange). The signal of H-34 correlates with the signal of C-8 (colored purple). In this way, connectivity among the prenyl units was established. Finally, the assignment to each  $\text{C}=\text{C}$  double bond of an *E* or *Z* configuration was determined by analyzing the ROESY spectrum. Figure 4C summarizes the  $^1\text{H}$  resonance

identities for 4. The complete  $^1\text{H}$  and  $^{13}\text{C}$  NMR resonance assignments for 4 are given in Table S2 in the Supporting Information.

$\text{Eu}(\text{hcf})_3$  likewise facilitated the NMR assignment of structure to 4B2 (derived from 7b). While the dispersion effect of  $\text{Eu}(\text{hcf})_3$  was less than that seen for 4, it was nonetheless sufficient for the NMR assignment of structure to 4B2.

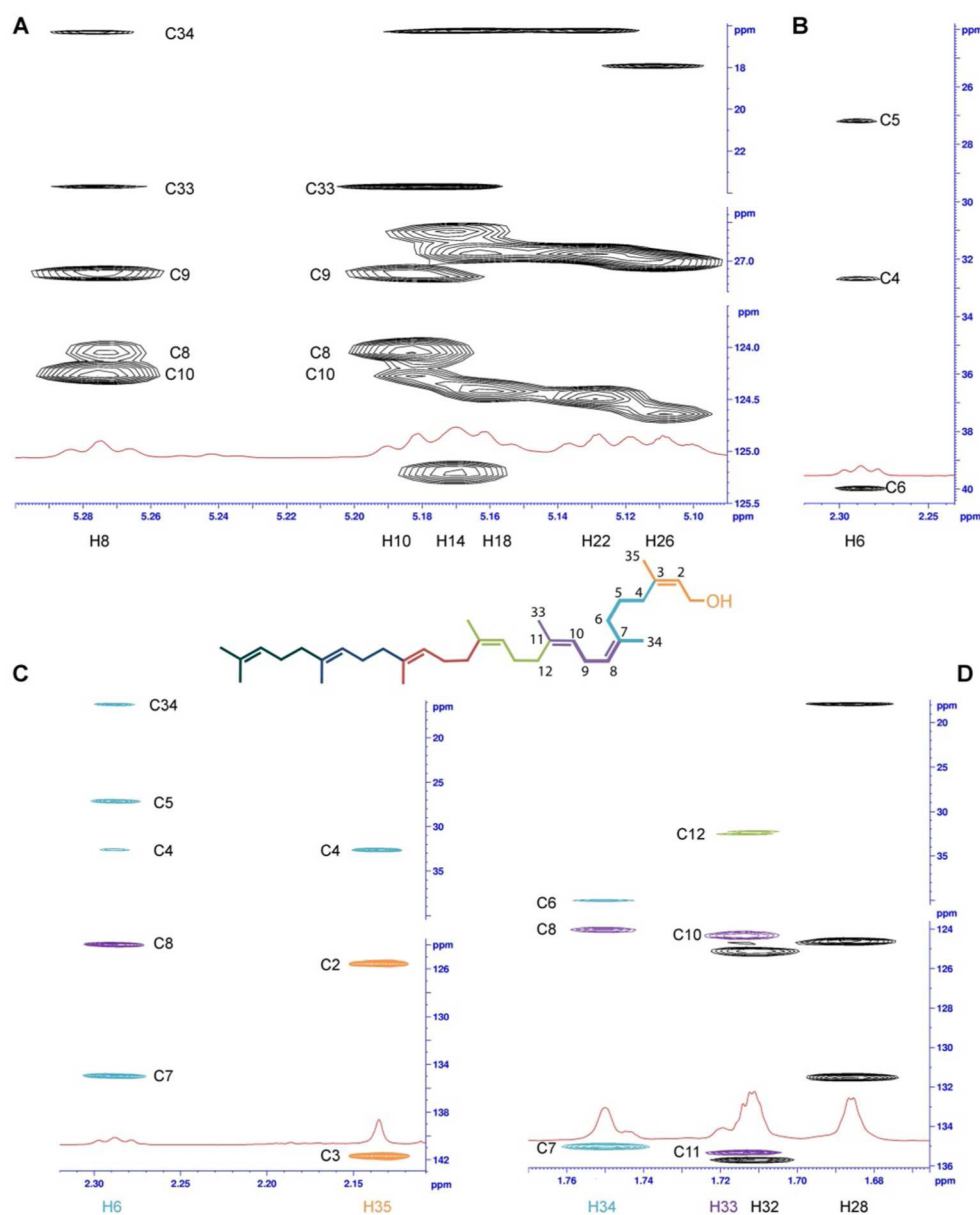


**Figure 5.** (A,B) HSQC-TOCSY and (C,D) HBMBC spectra of two atypical prenyl units of **4B2** (800.13 MHz, obtained using a solution of 10 mg of **4B2** and 3 mg of  $\text{Eu}(\text{hcf})_3$  in 600  $\mu\text{L}$  of  $\text{CDCl}_3$ ).

The structural difference occurs from C-5 to C-9 in **4B2**, giving two distinct and atypical units: one having three continuous  $\text{CH}_2$  carbons (C-4, C-5, and C-6) and the other having a single  $\text{CH}_2$  between two vinyl units (C-9 between C-8 and C-10). The two distinguishing resonances in the  $^1\text{H}$  spectrum of **4B2** (Figure 2) are those of H-5 and H-9. As a prenyl segment has a single vinyl hydrogen, there is always only one crosspeak in the vinyl  $^{13}\text{C}$  region of HSQC-TOCSY between vinyl proton and carbon resonances, which corresponds to a given vinyl CH group (see for example the crosspeak for the CH-6 vinyl group shown in Figure 4A). In contrast, the vinyl H-8 resonance of **4B2** shows in the same type of spectrum two crosspeaks: one with the vinyl C-8 resonance and the other with vinyl the C-10 resonance (Figure 5A). Similarly, the vinyl H-10 resonance also shows two crosspeaks: one with the vinyl C-10 resonance and the other with the vinyl C-8 resonance. Both H-8 and H-10 resonances then exhibit a crosspeak with the C-9 resonance at  $\delta = 27.19$

ppm, defining the first atypical unit. The second unit contains three consecutive  $\text{CH}_2$ 's (correlations are shown in Figure 5B). The HBMBC spectrum confirmed the proposed connectivities of the two atypical units: both connected to each other and between the first and fourth prenyl units (Figure 5C,D). Hence the terminal prenyl (colored orange) is connected to the  $-(\text{CH}_2)_3-$  segment (colored turquoise) as evidenced by the HMC correlation of the H-35 resonance with the C-4 resonance. Correlations of the H-6 and H-34 resonances with the C-8 resonance confirmed connection of the  $-(\text{CH}_2)_3-$  segment to the prenyl segment colored in purple. Finally, the crosspeak between the H-33 (purple unit) and C-12 resonances confirmed connectivity to the prenyl unit colored in green. The  $^1\text{H}$  and  $^{13}\text{C}$  resonance assignments for **4B2** are given in Table S2 in the Supporting Information.

An overall 30% yield of the 3:1 mixture of **4B2** and **4** (from prenyl sulfone **11**) characterized the failed route B. The two successful routes A and C to **4** gave comparable overall yields of

20% for route A and 18% for route C relative to their respective prenyl sulfones (**8** and **12**) as starting materials. In terms of heptaprenol yield the two routes are equivalent. A clear choice between the two routes emerges for the synthesis of longer polyprenols. After the first coupling reaction, route A requires transformation of the coupling product **18** to halide **19** via *O*-THP deprotection, followed by bromination. Route C requires transformation of the coupling product **22** to sulfone **24** via debenzoylation/detosylation, followed by bromination and subsequent tosylation. Overall, these three steps of route C are lower yielding (39%), as compared to the overall yield (69%) for the comparable steps of route A. For longer prenyls (polyprenols) route C is uncompetitive compared to route A, as route C will require iterative repetition of the lower-yielding steps.

## CONCLUSION

Polyprenols are the membrane-bound component of such a diversity of biosynthetic intermediates that they have been termed “superlipids”.<sup>37</sup> This diversity is exemplified by the recent syntheses, using both chemical and chemoenzymatic means, of the GlcNAc-UDP intermediate of bacterial cell wall biosynthesis;<sup>38</sup> of the glycosyl intermediates of bacterial *N*-linked glycosylation;<sup>27,39</sup> of bacterial teichoic acid biosynthesis;<sup>40</sup> of the Gram-positive bacterial *S*-layer glycan;<sup>41</sup> of the bacterial polysialic capsule;<sup>42</sup> and of the mycobacterial arabinan glyconjugates.<sup>43,44</sup> In all of these syntheses the prenyl is a mass-limiting reagent.

Herein we report a practical, multigram synthesis of the (*Z*<sub>4</sub>*E*<sub>2</sub>*ω*)-heptaprenol **4** as a key enabling material for the synthesis of these biosynthetic intermediates, and also including the Lipid II intermediate for peptidoglycan biosynthesis. The purity of **4** we obtain (>90%) is directly comparable to the purity of **4** that may be obtained by solid-phase synthesis.<sup>28</sup> The key advantage of our solution synthesis is its potential for scale. The pivotal intermediate **8** is prepared easily on a 30-g scale, and may be transformed to secure **4** on a >2-g scale.

Our optimized synthesis uses the classical retrosynthetic route (route A) for *Z*-prenyl homologation. Notwithstanding the precedence for route A, an unexpectedly facile and unusual rearrangement was encountered during allylic chlorination of a key intermediate, but not seen during allylic bromination of this same intermediate under otherwise identical experimental conditions. Our optimism that a better synthesis of **4** might be attained using a more accessible reagent pair in an alternate route (route B) was dashed by a facile isomerization that occurred during the reductive desulfonylation of a late-stage intermediate. These observations emphasize the necessity for rigorous proof of structure in prenyl synthesis, even following seemingly straightforward synthetic transformations. Here, proof of the latter isomerization and verification of the final (*Z*<sub>4</sub>*E*<sub>2</sub>*ω*)-heptaprenol structure of **4** used extensive two-dimensional NMR correlations in the presence of the chiral shift reagent Eu(hfc)<sub>3</sub> for resonance dispersion. The advantageous use of chiral shift reagents and high magnetic field strength as seen here for these prenyls suggests a general value to this approach for NMR structural assignment.

## EXPERIMENTAL SECTION

**NMR Spectroscopy.** The structures of prenyl **4** and **4B2** [10 mg of each was dissolved in 600 μL of CDCl<sub>3</sub> containing 3 mg of Eu(hfc)<sub>3</sub>] were determined by interpretation of the homonuclear DQF-COSY, TOCSY, and ROESY and heteronuclear <sup>1</sup>H–<sup>13</sup>C HSQC,

HSQC-TOCSY, and HMBC NMR spectra. Proton connectivities were derived from the DQF-COSY and TOCSY spectra. <sup>13</sup>C resonances corresponding to carbons with directly attached protons were assigned using HSQC and HSQC-TOCSY spectra. HMBC spectra were used to assign resonances of the quaternary carbons and to validate the connectivities established by the other spectra. ROESY spectra were utilized to establish the *E* or *Z* configurations for each C=C double bond. Experiments were performed at 25 °C using a Bruker AVANCE II spectrometer equipped with a TCI cryoprobe and operating at a <sup>1</sup>H resonance frequency of 800.13 MHz. Standard pulse sequences were used.<sup>45–50</sup> Time domain data (*t*<sub>2</sub> and *t*<sub>1</sub>) for 2D experiments were recorded as 2048 × 1024 complex matrices with 16 and 32 scans per *t*<sub>1</sub> increment for homonuclear and heteronuclear spectra, respectively. Relaxation delay between individual scans and spin-lock time for TOCSY experiments was 1.4 s and 60 ms, respectively. For ROESY experiments, a relaxation delay of 4 s and a spin-lock time of 400 ms gave 2048 × 512 complex time domain points. Linear prediction to 1024 complex points was applied in the *t*<sub>1</sub> domain. The data were zero-filled to obtain final 2048 × 2048 complex matrices. In all other homonuclear 2D experiments, zero-filling was used only in the *t*<sub>1</sub> domain to obtain final 2048 × 2048 complex time domain data. In heteronuclear 2D experiments, linear prediction to 2048 complex data points was employed in the *t*<sub>1</sub> domain, which was zero-filled to 4096 to get final 2048 × 4096 complex time domain data. Shifted sine bell weighting functions were applied in both domains prior to double Fourier transformation. In the 3D <sup>1</sup>H–<sup>13</sup>C HSQC-TOCSY experiments, 1024 × 48 × 128 complex time domain points in *t*<sub>3</sub>, *t*<sub>2</sub>, and *t*<sub>1</sub> domains were collected with 16 scans per time increment, relaxation delay of 1.3 s, and 60 ms spin-lock. Linear predictions to 128 and 256 complex points were utilized in the *t*<sub>2</sub> and *t*<sub>1</sub> domains. Zero-filling gave 2048 × 256 × 512 complex matrices. Shifted sine bell weighting functions were applied in all three domains prior to triple Fourier transformation. Spectra were processed using Bruker TopSpin 2.1 software. <sup>1</sup>H spectra, the <sup>1</sup>H dimension in 2D heteronuclear spectra, and the 1D <sup>13</sup>C{<sup>1</sup>H} spectra were referenced to solvent (DMSO, δ<sub>H</sub> 2.5 and δ<sub>C</sub> 39.5 ppm; CDCl<sub>3</sub>, δ<sub>H</sub> 7.27 and δ<sub>C</sub> 77.23 ppm). The <sup>13</sup>C dimension in the 2D heteronuclear spectra was referenced indirectly.<sup>51</sup>

## ASSOCIATED CONTENT

### Supporting Information

Experimental procedures and NMR data for all new compounds. This material is available free of charge via the Internet at <http://pubs.acs.org>.

## AUTHOR INFORMATION

### Corresponding Author

mobashery@nd.edu

### Notes

The authors declare no competing financial interest.

## ACKNOWLEDGMENTS

We thank Prof. Po-Huang Liang (Academia Sinica) for the clarification of the stereochemistry of the endogenous bacterial undecaprenol. This work was supported by a grant from the National Institutes of Health. The Mass Spectrometry & Proteomics Facility of the University of Notre Dame is supported by grant CHE-0741793 from the National Science Foundation.

## REFERENCES

- (1) Oldfield, E.; Lin, F.-Y. *Angew. Chem., Int. Ed.* **2012**, *51*, 1124–1137.
- (2) Hartley, M.; Imperiali, B. *Arch. Biochem. Biophys.* **2012**, *517*, 83–97.
- (3) Hug, I.; Feldman, M. *Glycobiology* **2011**, *21*, 138–151.

- (4) Chatterjee, A. N.; Park, J. T. *Proc. Natl. Acad. Sci. U.S.A.* **1964**, *51*, 9–16.
- (5) Meadow, P. M.; Anderson, J. S.; Strominger, J. L. *Biochem. Biophys. Res. Commun.* **1964**, *14*, 382–387.
- (6) Anderson, J. S.; Matsushashi, M.; Haskin, M. A.; Strominger, J. L. *J. Biol. Chem.* **1967**, *242*, 3180–3190.
- (7) Higashi, Y.; Strominger, J. L.; Sweeley, C. C. *Proc. Natl. Acad. Sci. U.S.A.* **1967**, *57*, 1878–1884.
- (8) Feeney, J.; Hemming, F. W. *Anal. Biochem.* **1967**, *20*, 1–15.
- (9) Tanaka, Y.; Hirasawa, H. *Chem. Phys. Lipids* **1989**, *51*, 183–189.
- (10) Chen, Y.; Chen, A.; Chen, C.; Wang, A.; Liang, P. *J. Biol. Chem.* **2002**, *277*, 7369–7376.
- (11) Lu, Y.; Liu, H.; Liang, P. *Biochem. Biophys. Res. Commun.* **2009**, *379*, 351–355.
- (12) Lu, Y.; Liu, H.; Teng, K.; Liang, P. *Biochem. Biophys. Res. Commun.* **2010**, *400*, 758–762.
- (13) Teng, K.; Liang, P. *Bioorg. Chem.* **2012**, *43*, 51–57.
- (14) Barreteau, H.; Magnet, S.; El Ghachi, M.; Touze, T.; Arthur, M.; Mengin-Lecreulx, D.; Blanot, D. *J. Chromatogr. B: Anal. Technol. Biomed. Life Sci.* **2009**, *877*, 213–220.
- (15) van Heijenoort, J. *Microbiol. Mol. Biol. Rev.* **2007**, *71*, 620–635.
- (16) Auger, G.; Crouvoisier, M.; Caroff, M.; van Heijenoort, J.; Blanot, D. *Letts. Pept. Sci.* **1997**, *4*, 371–376.
- (17) Dumbre, S.; Derouaux, A.; Lescrier, E.; Piette, A.; Joris, B.; Terrak, M.; Herdewijn, P. *J. Am. Chem. Soc.* **2012**, *134*, 9343–9351.
- (18) VanNieuwenhze, M. S.; Mauldin, S. C.; Zia-Ebrahimi, M.; Winger, B. E.; Hornback, W. J.; Saha, S. L.; Aikins, J. A.; Blaszcak, L. C. *J. Am. Chem. Soc.* **2002**, *124*, 3656–3660.
- (19) Ye, X.-Y.; Lo, M.-C.; Brunner, L.; Walker, D.; Kahne, D.; Walker, S. *J. Am. Chem. Soc.* **2001**, *123*, 3155–3156.
- (20) Zhang, Y.; Fechter, E. J.; Wang, T.-S. A.; Barrett, D.; Walker, S.; Kahne, D. E. *J. Am. Chem. Soc.* **2007**, *129*, 3080–3081.
- (21) Schwartz, B.; Markwalder, J. A.; Wang, Y. *J. Am. Chem. Soc.* **2001**, *123*, 11638–11643.
- (22) VanNieuwenhze, M. S.; Mauldin, S. C.; Zia-Ebrahimi, M.; Aikins, J. A.; Blaszcak, L. C. *J. Am. Chem. Soc.* **2001**, *123*, 6983–6988.
- (23) Liu, C.-Y.; Guo, C.-W.; Chang, Y.-F.; Wang, J.-T.; Shih, H.-W.; Hsu, Y.-F.; Chen, C.-W.; Chen, S.-K.; Wang, Y.-C.; Cheng, T.-J. R.; Ma, C.; Wong, C.-H.; Fang, J.-M.; Cheng, W.-C. *Org. Lett.* **2011**, *12*, 1608–1611.
- (24) Gampe, C. M.; Tsukamoto, H.; Wang, T.-S. A.; Walker, S.; Kahne, D. *Tetrahedron* **2011**, *67*, 9771–9778.
- (25) Inoue, S.; Kaneko, T.; Takahashi, Y.; Miyamoto, O.; Sato, K. *J. Chem. Soc., Chem. Commun.* **1987**, 1036–1037.
- (26) Sato, K.; Miyamoto, O.; Inoue, S.; Matsushashi, Y.; Koyama, S.; Kaneko, T. *J. Chem. Soc., Chem. Commun.* **1986**, 1761–1762.
- (27) Lee, J.; Ishiwata, A.; Ito, Y. *Tetrahedron* **2009**, *65*, 6310–6319.
- (28) Chang, Y.-F.; Liu, C.-Y.; Guo, C.-W.; Wang, Y.-C.; Fang, J.-M.; Cheng, W.-C. *J. Org. Chem.* **2008**, *73*, 7197–7203.
- (29) Sato, K.; Miyamoto, O.; Inoue, S.; Furusawa, F.; Matsushashi, Y. *Chem. Lett.* **1983**, 725–728.
- (30) Misiak, M.; Koźmiński, W.; Kwasiborska, M.; Wójcik, J.; Ciepichal, E.; Swiezewska, E. *Magn. Reson. Chem.* **2009**, *47*, 825–829.
- (31) Heldman, D.; Gilde, H.-G. *J. Chem. Educ.* **1980**, *57*, 390–391.
- (32) Wenzel, T. J.; Chisholm, C. D. *Prog. Nucl. Magn. Reson. Spectrosc.* **2011**, *59*, 1–63.
- (33) Baldovini, N.; Tomi, F.; Casanova, J. *Magn. Reson. Chem.* **2001**, *39*, 621–624.
- (34) Blanc, M.-C.; Bradesi, P.; Casanova, J. *Magn. Reson. Chem.* **2005**, *43*, 176–179.
- (35) Ghosh, I.; Kishi, Y.; Tomoda, H.; Omura, S. *Org. Lett.* **2004**, *6*, 4719–4722.
- (36) Lanfranchi, D.; Blanc, M.-C.; Vellutini, M.; Bradesi, P.; Casanova, J.; Tomi, F. *Magn. Reson. Chem.* **2008**, *46*, 1188–1194.
- (37) Surmacz, L.; Swiezewska, E. *Biochem. Biophys. Res. Commun.* **2011**, *407*, 627–632.
- (38) Al-Dabbagh, B.; Blanot, D.; Mengin-Lecreulx, D.; Bouhss, A. *Anal. Biochem.* **2009**, *391*, 163–165.
- (39) Hartley, M.; Larkin, A.; Imperiali, B. *Bioorg. Med. Chem.* **2008**, *16*, 5149–5156.
- (40) Brown, S.; Zhang, Y.; Walker, S. *Chem. Biol.* **2008**, *15*, 12–21.
- (41) Holkenbrink, A.; Koester, D.; Kadchel, J.; Werz, D. *Eur. J. Org. Chem.* **2011**, *2011*, 6233–6239.
- (42) Shpirt, A.; Kononov, L.; Maltsev, S.; Shibaev, V. *Carbohydr. Res.* **2011**, *346*, 2849–2854.
- (43) Liav, A.; Ciepichal, E.; Swiezewska, E.; Bobovská, A.; Dianišková, P.; Blaško, J.; Mikušová, K.; Brennan, P. *Tetrahedron Lett.* **2009**, *50*, 2242–2244.
- (44) Zhang, J.; Angala, S.; Pramanik, P.; Li, K.; Crick, D.; Liav, A.; Jozwiak, A.; Swiezewska, E.; Jackson, M.; Chatterjee, D. *ACS Chem. Biol.* **2011**, *6*, 819–828.
- (45) Bax, A.; Morris, G. A. *J. Magn. Reson.* **1981**, *42*, 501–505.
- (46) Bax, A.; Summers, M. F. *J. Am. Chem. Soc.* **1986**, *108*, 2093–2094.
- (47) Bodenhausen, G.; Freeman, R.; Niedermeyer, R.; Turner, D. L. *J. Magn. Reson.* **1977**, *26*, 133–164.
- (48) Griesinger, C.; Otting, G.; Wüthrich, K.; Ernst, R. R. *J. Am. Chem. Soc.* **1988**, *110*, 7870–7872.
- (49) Sattler, M.; Schwalbe, H.; Griesinger, C. *J. Am. Chem. Soc.* **1992**, *114*, 1126–1127.
- (50) Wijmenga, S. S.; Hallenga, K.; Hilbers, C. W. *J. Magn. Reson.* **1989**, *84*, 634–642.
- (51) Wishart, D. S.; Bigam, C. G.; Yao, J.; Abildgaard, F.; Dyson, H. J.; Oldfield, E.; Markley, J. L.; Sykes, B. D. *J. Biomol. NMR* **1995**, *6*, 135–140.